Available online at www.sciencedirect.com
SCIENCE DIRECT®
Polymer 44 (2003) 6241–6250
polymer
www.elsevier.com/locate/polymer

Fire retardancy of polypropylene/flax blends

B. Schartel[a,*], U. Braun[a], U. Schwarz[b], S. Reinemann[c]

[a]*Federal Institute for Materials Research and Testing, Unter den Eichen 87, 12205 Berlin, Germany*
[b]*Ostthüringische Materialprüfgesellschaft für Textil und Kunststoffe mbH Rudolstadt, Breitscheidstraße 97, 07407 Rudolstadt, Germany*
[c]*Thüringisches Institut für Textil- und Kunststoff-Forschung e.V., Breitscheidstraße 97, 07407 Rudolstadt, Germany*

Received 27 January 2003; received in revised form 3 July 2003; accepted 23 July 2003

Abstract

A comprehensive characterization of the thermal and the fire behaviour is presented for polypropylene (PP) flax compounds containing ammonium polyphosphate (APP) and expandable graphite as fire retardants. Thermogravimetry coupled with an evolved gas analysis (TG-FTIR) was performed to ensure a significant thermal analysis. The fire response under forced flaming conditions was studied using a cone calorimeter. The external heat flux was varied between 30 and 70 kW m^{-2} so that the results could be evaluated for different fire scenarios and tests. Different flammability tests (UL 94, limiting oxygen index, glow wire test, GMI 60261) were performed and the results compared with the cone calorimeter data. The different char forming mechanisms are described and the resulting fire retardancy is classified. The successful and ecological friendly fire retardancy is a technological breakthrough for PP/flax biocomposites.

Keywords: Biocomposites; Flame retardancy; Flax

1. Introduction

Many natural polymers are highly optimised functional and structural materials that are suited in principle for technical applications. It is worth noting that natural materials optimisation is different in principle than human synthetic approaches [1]. Natural structural materials, for instance, are built up by means of growth and in a hierarchical way. Therefore, nature extensively exploits self-organization on the nanoscale while obliterating the boundaries between construction and material. Furthermore, since they are renewable, using natural materials can save valuable resources. Additionally, at the end of product lifecycle, natural polymers can reduce problems to a certain extent, due to their biodegradability. A major problem for industrial exploration is processing in the molten state. Therefore, blending synthetic and natural polymers is an interesting approach [2–4]. Such biocomposites are discussed for different applications. Today biocomposites thus are used for a wide range of products, such as construction and insulation panels made of wood pieces, special textiles, composites based on polymer filled with lignocellulosic particles, fibres and membranes. In particular, using natural fibres for polymer composites exhibits the most potential benefits for making natural/synthetic polymer blends of industrial value [5–7].

Producing lightweight structural components is a key challenge for high technology industries like automotive and aircraft construction. Consequently, steel alloys are more and more replaced by aluminium, plastics and composites. Natural fibre composites are recognized as a realistic alternative to conventional glass-reinforced composites. In fact, natural fibres like flax and sisal are fast-growing additives for thermoplastics. Key advantages of natural fibres over traditional reinforcing fibres such as glass and carbon are: low cost, low density and the fact that they are recyclable. One of the limitations of lignocellulosic fibres is that a relatively low processing temperature (up to about 475 K) is required in order to avoid decomposition. Consequently, the suitable polymer matrix materials are restricted to thermoplastics with corresponding low processing temperatures such as polyethylene (430–570 K [8]), polypropylene (475–540 K [8]), polyvinyl chloride (450–480 K [8]) and polystyrene (450–550 K [8]), which are fortunately the most common used polymers. Consequently,

* Corresponding author. Tel.: +49-30-8104-1021; fax: +49-30-8104-1037.
E-mail address: bernhard.schartel@bam.de (B. Schartel).

0032-3861/$ - see front matter © 2003 Elsevier Ltd. All rights reserved.
doi:10.1016/S0032-3861(03)00692-X

a major focus is on the development of polypropylene (PP) composites with bast fibres such as flax [9–11].

Besides the main properties for structural materials, mechanical properties and the material costs, for many applications fire behaviour is important. Recently, the flammability of PP composites with long flax fibres was investigated by varying the fibre content [12]. A fibre content of 12.5% was reported to work as a kind of fire retardant. For a higher content, the fire behaviour seems to change to the typical fire response for a lignocellulosic material. Very recently, PP-flax compounds including different flame retardants were proposed [13], which fulfil the industrial demands on processing and mechanical properties. Expandable graphite and ammonium polyphosphate were used as flame retardants.

Monoammonium phosphate and diammonium phosphate are used as flame retardants in a variety of cellulosic materials [14,15]. They function by increasing the amount of char. They decompose to phosphoric acid, which esterifies the hydroxyl groups. The resulting cellulose ester increases the char amount of the decomposition [14,15]. Ammonium polyphosphate is water-insoluble, non-melting solid with high phosphorus content used in intumescent coatings. Ammonium polyphosphate, especially in combination with char forming, nitrogen-containing compounds, is an effective fire retardant and common in polypropylene materials [14,16,17,18].

Expandable graphite increasingly is being discovered as an effective flame retardant. It is environment friendly, water insoluble, and functions as a flame retardant by endothermic combustion reaction, but especially thanks to its enormous expansion. In fact, it expands under the impact of heat to up to 300 times of its initial volume and creates a very large surface [19]. A quick oxidation of the carbon occurs, consuming the oxygen so that flames are smothered in the event of a fire. The oxidation of the graphite itself is not a source of fire, since it does not create flames during oxidation. The expansion creates a heat insulating layer as well as reducing dripping problems. Expandable graphite is also known to be an effective smoke suppressant.

It is the aim of this paper to give deeper and more comprehensive insight into the fire behaviour and fire retardancy of PP-flax fibre composites containing ammonium polyphosphate and expandable graphite, respectively. Thermal analysis, cone calorimeter investigations and flammability tests were performed.

2. Experimental

2.1. Materials

The polypropylene (PP) was H715-12 (Dow Plastics, Switzerland). The material flow properties of this homopolymer are suitable for injection moulding. The flax fibre was added by using flax mat Ref DI 263 (Saneco, France). Exolit® AP 751 (TP) (Clariant, Germany) was used as an ammonium polyphosphate (APP) based fire retardant. The commercial product is actually a mixture of APP comprising around two-thirds and different synergistic materials. The phosphorus content is around 22.5 wt% (according to ISO 3706) and the nitrogen content 13 wt% (according to Kjeldahl). The expandable graphite (EG) was Nord-Min® Type 250 (Nordmann, Germany). This type of expandable graphite is based on sulphuric acid modification and is characterized by a 250-fold free expansion starting at around 470 K. For the thermal decomposition, 17.46 wt% are reported as volatile products. The compounds were prepared using a double screw extruder ZSK 40 (Werner & Pfeiderer, Germany) with a rotational speed of 300 min^{-1} and a throughput of 30 kg h^{-1}. The temperature profile was 473/473/463/443/453/443/453/453/483 K along the extruder from the feeder to the nozzle. Vacuum was applied. Injection moulding using an Allrounder 320M 500-210 (Arburg, Germany) was performed to manufacture test pieces according to ISO 294. The temperature profile was 353/453/458/463/468 K along the injection moulding machine from the feeder to the nozzle and the injection pressure was 800 bar. For the cone calorimeter measurements 100 × 100 × 5 mm plates were pressed from granulate. The temperature was 473 K; the pressure was 200 bar, and the time intervals were 6 min heating and 13 min cooling. The different compounds investigated are summarized in Table 1.

2.2. Thermal analysis

A TGA/SDTA 851 (Mettler-Toledo, Germany) coupled with a FTIR-Spectrometer Nexus 470 (Nicolet, Germany) was used to perform the thermogravimetric-Fourier transform infrared (TG-FTIR) experiments. The measurements were performed in the temperature range of 298–1100 K with a heating rate of 10 K min^{-1} and a nitrogen flow of 30 ml min^{-1}. Chips were cut from cone calorimeter plates and around 10 mg samples were used for the experiments. All measurements were done in duplicate showing a good reproducibility. The averaged values were discussed as results and the deviation between the two measurements were used to estimate the error. A transfer line consisting of a glass-coated tube heated at 473 K connected the TG to an infrared gas cell heated at 483 K. The FTIR is equipped with a DTGS KBr detector and operated in the mid-infrared

Table 1
Composition of the investigated materials

Sample	PP content (wt%)	Flax fibre content (wt%)	Exolit® content (wt%)	EG content (wt%)
V2 FL30	70	30		
V8 APS25	45	30	25	
V5 G15	55	30		15
V5 G25	45	30		25

range (400–4000 cm^{-1}) with an optical resolution of 4 cm^{-1}. The evolution of the FTIR characteristics was monitored against the time. The spectra, which correspond to the maximum mass loss rates, are chosen to identify the evolved gases.

2.3. Cone calorimeter

Cone calorimeter (Fire Testing Technology, UK) investigations were performed on the fire behaviour according to ASTM E 1354/ISO 5660. External heat fluxes of 30, 40, 50 and 70 kW m^{-2} were applied. All of the samples were measured in the horizontal position. A retainer frame was used to reduce unrepresentative edge burning; decreased sample area was taken into account for data evaluation. All measurements were done in duplicate. The reproducible visual determination of the flameout turned out to be difficult, since some samples show very small flame zone extension or significant afterglow, respectively. Therefore, the flameout was determined as the intersection of the tangent at the trailing edge of the heat release rate with the abscissa. Measures such as total heat release (THR) and mass loss are discussed for that time point and marked with (t), for instance THR (t) in Figs. 4–6.

2.4. Flammability tests

The flammability of the different samples was characterized using four different tests: the limiting oxygen index (LOI), UL 94, GMI 60261 (burning behaviour of interior materials of vehicles) and a glow wire test. The LOI was determined according to ISO 4589. The materials were classified according UL 94 using 3.2 mm thick samples. With respect to application in vehicles, the flammability was described using the test method for determining the flammability of interior trim materials according to GMI 60261. The glow wire flammability index was monitored according to IEC 695 (2-1).

3. Results and discussion

3.1. Thermal analysis

The results of the thermal analysis are shown in Fig. 1. All materials decomposed in two decomposition steps. Table 2 summarizes the characteristics for the two subsequent decomposition steps. For all the materials, the first step is attributed to the decomposition of flax, the second one to the decomposition of PP. This assignment considers the results for the distinct steps with respect to mass loss, temperature interval and evolved gas analysis. In the case of V2 FL30, around 78 wt% of the flax is decomposed in the first step, and around 91 wt% of the PP in the second step. The residue at higher temperatures is around 13.8 wt%. The temperature intervals for the two

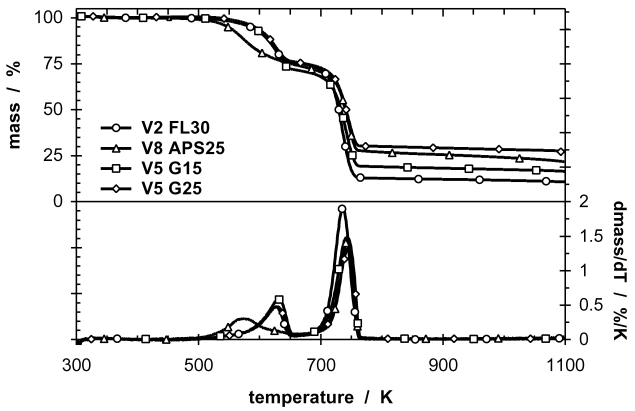

Fig. 1. TG for the different samples under N_2, heating rate 10 K min^{-1}.

decomposition steps correspond well to the decomposition temperatures reported for cellulose (550–650 K) and PP (590–710 K), respectively [20]. Fig. 2 displays the FTIR spectra for the two maxima of mass loss. The FTIR spectra are dominated by absorption characteristics which correspond to the typical decomposition products of cellulose and PP, respectively [21]. For the mass loss rate maximum of the first steps, the simultaneously evolved gas analysis proves the occurrence of characteristic absorption in the regions of around 3400–4000 cm^{-1}, around 2700–3000 cm^{-1}, around 2250–2400 cm^{-1}, around 1600–1900 cm^{-1}, around 1250–1600 cm^{-1} and around 1100 cm^{-1}. The spectrum fits well to the reported FTIR features of typical decomposition products of cellulose, especially the low molecular weight gas products such as CO_2 (2250–2400 cm^{-1}), H_2O (3400–4000 cm^{-1} and 1200–2200 cm^{-1}), hydrocarbons (2800–3000 cm^{-1}) and CH_2O (CH stretching ~2782 cm^{-1}; C=O stretching ~1746 cm^{-1}), but also other C–H stretching at ~1500, ~2843, ~1249 and ~1167 cm^{-1}) [22,23]. The FTIR spectrum for the second mass-loss rate maximum is dominated by the absorption bands around 3079 cm^{-1}, around 2820–3020 cm^{-1}, around 1635–1655 cm^{-1} around 1340–1510 cm^{-1}, and around 900 cm^{-1}. The spectrum

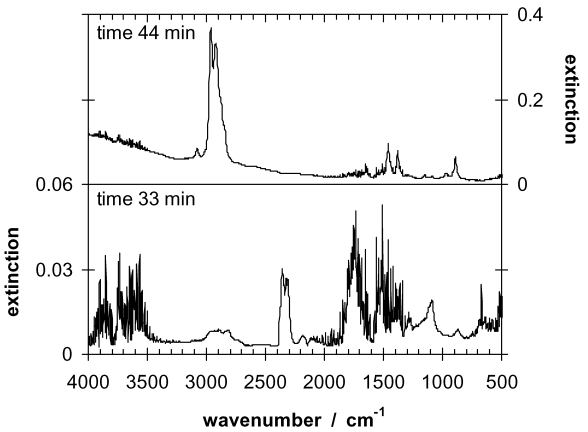

Fig. 2. FTIR spectra at the maximum mass loss rate of the first and second decomposition steps for V2 FL30.

Table 2
TG results

Sample	V2 FL 30	V8 APS25	V5 G15	V5 G25
Sample weight (mg)	9.3 ± 0.5	10.1 ± 0.5	11.4 ± 1.0	9.3 ± 1.0
T_{DTGmax} (1st step) (K)	627.5 ± 1.0	573.2 ± 2.0	630.8 ± 0.5	626.9 ± 0.5
Mass loss (1st step) (%)	23.4 ± 1.5	24.1 ± 2.0	28.5 ± 0.5	25.5 ± 1.0
T_{DTGmax} (2nd step) (K)	735.7 ± 0.5	745.4 ± 0.5	740.8 ± 0.5	744.5 ± 0.5
Mass loss (2nd step) (%)	62.2 ± 0.5	48.9 ± 2.0	53.7 ± 1.5	45.6 ± 0.5
Residue at 765 K (%)	13.9 ± 1.0	27.4 ± 0.5	18.3 ± 1.0	29.4 ± 1.0
Cone calorimeter residue at $t_{flameout}$ (%)	10.6 ± 2.0	29.3 ± 2.0	28.4 ± 4.0	(>29.6 ± 4.0)

corresponds to the reported FTIR features of the decomposition products of PP-saturated and unsaturated hydrocarbons typically in the C_1–C_7 range, with propylene, C_5 and C_6 being the main products [24,25]. The typical absorptions for such products are reported with CH_2/CH_3 stretching (~2860–2970 cm^{-1}), C=C stretching (~1661 cm^{-1}), asymmetric CH_3 bending (1452–1465 cm^{-1}) or symmetric CH_3 bending (1372–1381 cm^{-1}).

Adding 25 wt% APP-based flame retardant (V8 APS25) accelerates the first step of decomposition. The temperature for the maximum mass loss is around 54 K below the temperature without APP. Hence, the temperature interval for the first decomposition step does not only correspond to the decomposition of the cellulose, but is also typical for the release of NH_3 from the APP [26]. However, the mass loss of the first step is approximately equal for V2 FL30 and V8 APS25. This may be explained by the fact, that the expected mass loss due to the release of NH_3 is in the same order of magnitude as the errors of the mass loss determination. Furthermore, already a small increase of the char yield due to the flax decomposition may compensate the effect in terms of mass loss. The residue of the first step contains PP decomposing in the subsequent second decomposition step and char. This char results in part from the decomposed flax, and in part is composed of the APP-based additive. The latter is expected to show heat insulation properties, so that it is not surprising that the second decomposition step is shifted (around 10 K) to higher temperatures. It should be noted that the observed influence of APP on the system is comparable to the function of APP in other materials such as polyamide/ethylene-vinyl-acetat, polyurethane, or ethylene–propylene rubber/polyurethan [27,28,29]. For instance, APP is also reported to accelerate the decomposition but leads to an increase in the amount of high-temperature residue, which acts as a protective thermal barrier. In the second step, decomposition of the PP content is observed but also a further decomposition of the products based on the flax and fire retardant additive, which is illustrated by the mass loss and the additional products such as H_2O. Therefore, the amount of high temperature residue after the second decomposition, around 27.4%, corresponds to the sum of around 13.7 wt% char which corresponds to the char amount found for V2 FL30, and an additional residue around 13.7 wt%. This residue due to the APP-based additive, largely corresponds to highly cross-linked phosphorus oxides or phosphates, respectively [30,31]. The probable phosphorus/oxygen or phosphorus/(oxygen + nitrogen) content, respectively, of the residue is around 2:5. The exact nitrogen content in the residue is unclear, since the study does not reveal how much nitrogen is released as NH_3 and how much nitrogen remains in the residue, respectively.

Adding expandable graphite enhances the char formation during the first step, but does not influence its decomposition temperature interval significantly. The temperature of the second decomposition is shifted around 5 K and around 9 K for V5 G15 and V5 G25, respectively. These shifts are due to the thermal-insulation properties of expanded graphite. The residue after the second step is the sum of the char made up of flax and PP and the high temperature residue of the expandable graphite. The latter contribution is estimated at around 12.4 wt% for V5 G15 and around 20.7 wt% for V5 G25, respectively, considering the partial volatility of this filler. This mass loss of the expandable graphite can be attributed mainly to the decomposition of the sulphuric acid in the second decomposition step [26]. Hence, the materials V5 G15 and V5 G25 are characterized by an enhanced decomposition of the PP and flax content. In comparison to V2 FL30 (13.8 wt% residue from flax and PP) and V8 APS25 (13.7 wt% residue from flax and PP) only around 6 wt% and around 9 wt% residue from flax and PP are estimated for V5 G15 and V5 G25, respectively. The interaction between cellulose and the sulphuric acid of the expandable graphite is proposed to be the reason for this behaviour. It has been reported that the interaction between cellulose and sulphuric acid increases the yield of tar or levoglucosan, respectively, and decreases the yield of char [32]. The increase in the amount of tar corresponds to the decreased mass loss observed for the first step, whereas the decrease of char yield corresponds to the reduced high temperature residue detected.

3.2. Fire behaviour: visual observation for the forced flaming conditions in the cone calorimeter

V2 FL30 combusts to a rigid black residue, which cracks, glows and decomposes to white ash after the breakdown of a covering flame zone at the end of the experiment. The

charring behaviour is best described by comparing it to what is observed for burning wood. Indeed, since PP combusts with no significant residue, the flax fibres are the origin of the residue, in accordance with their lignocellulosic structure. In contrast to the pure PP matrix, the composites are char forming materials. At the end of the experiment, oxygen reaches the surface of the materials and the organic char is oxidized to white ash. V8 APS25 combusts to a rigid black residue which starts to glow at the end of the experiment. At first glance, the visual observations for V8 APS25 and V2 FL30 are very similar, but the flame zone during the experiment seems to be decreased moderately and the glowing of the char at the end of the experiment is changed slightly. No dominant oxidation of the char is observed. Hence, the properties of the char layer are changed due to a changed chemical composition. It can be assumed that the organic carbon char is accompanied by a more inorganic residue. V5 G15 and V5 G25 combust to a black, intumescent, loose residue. It is composed of thousands of wormlike structures rising at the surface, resulting in an extremely large surface area. The increasing sample size (thickness > 3 cm) results in a significant reduction of the distance to the cone heater; in fact, the material grows inside it. The flame extension is reduced drastically in comparison to the other materials. In fact, during the experiment the transition from burning with a flame to glowing without a flame is nearly continuous. The whole material is transformed to the loose wormlike residue. Especially, for V5 G25, some of these residue particles fall down softly. Hence, the sample mass during combustion is not only determined by the formation of volatile decomposition products but is also spoiled by an additional mass loss. Consequently, we will refrain from evaluating data based on inaccurate mass loss determination, so that for instance the calculation of THR per mass loss is not discussed for V5 G25 in the following.

3.3. Fire behaviour: fire risks for the forced flaming conditions in the cone calorimeter

Obviously, ignition and heat release are key features in respect to fire hazards and are discussed in the following using the term: fire risks. Fig. 3 shows the heat release rate and the THR plotted against the time during the performed cone calorimeter experiments. Fig. 3(a)–(c) show the heat release rate and the THR curves varying the external heat flux for the samples V2 FL30, V8 APS25 and V5 G15, respectively. For each external heat flux (30,40,50,70 kW m^{-2}) only one of the two measurements performed for each material is plotted. Fig. 3(d) shows the comparison of the different materials for an external heat flux of 40 kW m^{-2}. The illustrations of data for V5 G25 varying the external heat flux are not shown, since it can be imagined analogous to Fig. 3(c), taking into account the increased graphite content. The comparison of the different materials for 30, 50 and 70 kW m^{-2} were also not shown, since they can be imagined analogous to Fig. 3(d) taking into account the different external heat flux. The heat release rate and THR curves plotted against the experimental time show significant quantitative and qualitative deviations. For all the samples, the heat release rates increase with increasing external heat flux, whereas the burning time and the time to ignition decreases. Obviously, this is in accordance with the expected fire behaviour for different external heat fluxes. With increasing external heat fluxes the energy impact per time in the sample is increased. Therefore, the heating rate of the sample before reaching the ignition temperature is increased, which obviously results in a shorter time to ignition. After ignition, the increasing impact enlarges the decomposition, resulting in an increased fuel production rate. Consequently, the heat-release rate increases during burning and the time needed for a complete consumption of the polymeric material is shortened. The THR slightly increases with increasing external heat flux. The progress of the heat release rate during burning is different for the different materials. V2 FL30 shows two peaks for the heat release rate: one peak at the beginning of burning, when the formation of a char layer stops the initial increase after the ignition of unprotected material. The other peak is at the end, when the char cracks or the thermal feedback of the sample holder leads to an increasing volume of the pyrolysis zone. Both the double peak behaviour and the visually observed charring behaviour show similarity to the behaviour known for wood [33], as can be expected for the high flax content of 30 wt% [12]. The larger the external heat flux, the more pronounced the peaks are. Hence, it can be concluded that only for smaller heat flux are the samples thermally thick enough to adjust to a steady heat release rate, as is indicated for the measurement with 30 kW m^{-2}. V8 APS25 shows a typical heat release rate curve for a kind of char forming material, where the char influences the amount of combustible material and works as a barrier between the pyrolysis and flame zone. In fact, they are perfectly similar, for instance, to glass reinforced–reinforced polyamides containing red phosphorus [34,35], which convert the polyamide to such a char forming material. The initial increase is stopped by the formation of an effective char layer; a peak of the heat release rate is formed, probably because the barrier properties become dominant. Afterwards a region is found with a rate that is similar to steady heat release, characterized by a slightly decreasing heat release rate. There is a strong decrease in the heat release rate when the material is consumed accompanied with the flameout. The heat release curves of V5 G15 and V5 G25 can be understood as a superposition of two characteristics. First, the typical curve of a char forming material with steadily increasing barrier properties: the initial increase is stopped at the maximum of the heat release rate followed by a steady decrease of the heat release rate down to zero. Second, an experimental artefact: unfortunately, the intumescent behaviour lifts more and more material inside the cone, so that significant parts of

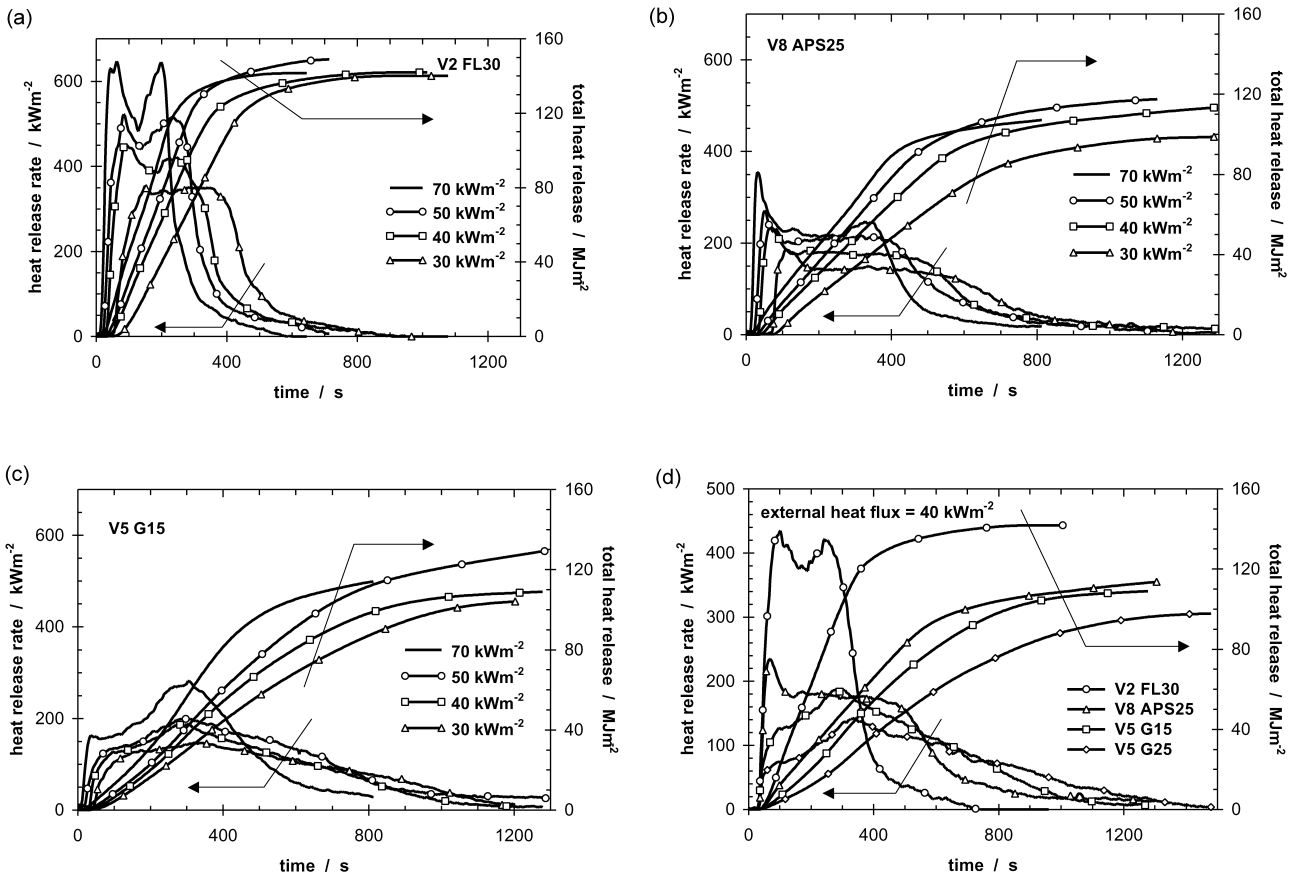

Fig. 3. (a) Heat release rate and the total heat release for the samples V2 FL30, varying the external heat flux (30,40,50,70 kW m^{-2}). (b) Heat release rate and the total heat release for the samples V8 APS25, varying the external heat flux (30,40,50,70 kW m^{-2}). (c) Heat release rate and the total heat release for the samples V5 G15, varying the external heat flux (30,40,50,70 kW m^{-2}). (d) Heat release rate and the total heat release for an external heat flux of 40 kW m^{-2} for the samples V2 FL30, V8 APS25, V5 G15 and V5 G25.

the material are exposed to higher heat fluxes, resulting in a higher conversion rate. This effect makes up a second peak characteristic, which was found to occur around 300 s. Before the different char layers are built up, all of the materials react similarly to the heat threat. Hence, the times to ignition and the initial increases in the heat release rate are quite comparable. Only for lower external heat fluxes like 30 and 40 kW m^{-2} does an increase in time to ignition become significant, especially for V8 APS25 and V5 G25. There is no obvious correlation between the differences in time to ignition and the different characteristics of the first decomposition step described for the materials. Neither the changes of the temperature interval nor the different mass loss during the first decomposition step are really capable of explaining the increase in time to ignition. Assuming that the ignition to stable burning occurs only if a pyrolysis temperature is reached, at which a decomposition including both decomposition steps takes place, it is quite probable that the materials show an improvement in time to ignition according to the reduction of the PP content. Hence, it is concluded that this effect is caused by a dilution effect. This interpretation corresponds well with a recently presented model for the ignition of char forming materials [36]. The similar and strong initial increase in heat release rate is stopped by the formation of char layer for all materials at quite similar times but at very different heat release rates. Hence, the materials are expected to show strongly decreasing fire growth rates in the order: V2 FL30, V8 APS25, V5 G15 and V5 G25. The quantitative comparison of the different materials clearly show decreased heat release rates and increased burning times, both of which are typical for an improved barrier property of the charring layer. Additionally, the THR is decreased according to the decreased amount of fuel fed to the flame zone.

In Fig. 4, the two most important characteristics for the fire risks, peak of the heat release rate and THR, are shown plotted against the external heat flux. The peak of the heat release rate, which is known to determine the fire risk flame spread, increases linearly with increasing external heat flux. The THR is nearly constant against the external heat flux for each of the materials V2 FL30, V8 APS25 and V5 G15. The slight increase, which is in the same order of magnitude as the error for the THR, is probably due to a slightly improved conversion of the material or a decreased residue under the protecting edge frame. Only the THR values of V5 G25 for 30 kW m^{-2} do not fit this description. Their total mass loss,

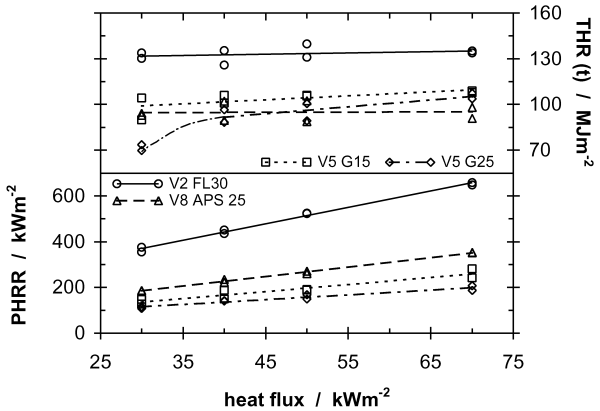

Fig. 4. Peak of the heat release rate (PHRR) and total heat release at the flame out (THR(t)) plotted against the external heat flux for the different materials.

and therefore their THR, is significantly smaller than the value one can expect from the measurement at higher external heat fluxes. It must be concluded that for these experimental parameters the thermal barrier is efficient enough to result in partially incomplete decomposition of the material. Comparing the data for the different materials, it is obvious that the peak of the heat release and THR are determined by the same fire retardancy effects which already were outlined for corresponding heat release curves against the experimental time. The replacement of PP by ammonium polyphosphate or graphite, respectively, results in a decrease of the THR. The barrier properties of the char layer determine the peak of the heat release rate. All materials are char forming systems, but the protection significantly increases for V8 APS25, V5 G15 and V5 G25 in comparison to V2 FL30. Additionally, the fire retardancy effect in terms of the peak of the heat release rate becomes more pronounced for higher external heat fluxes, as is typical for char forming materials [37].

The residues at flameout of each material were averaged for the measurements and were compared to the TG results (Table 2). The values show a good correspondence for V2 FL30 and V8 APS25. This result accords to general observation, that char yields for flaming combustion correspond to anaerobe pyrolysis simulated in the thermogravimetry [38]. Consequently, for both materials a total and anaerobe decomposition is concluded in the flaming combustion. The residue is constituted of the char, which stems from the flax, and, in the case of the V8 APS25 material, an additional residue which originates from the APP. Of course, adding expandable graphite also results in an additional residue, but no good correspondence was found between the residue in the TG and in the burning experiment. The residue characteristic for the burning experiment clearly exceeds the one for TG. Hence a partly aerobe pyrolysis occurs or the thermal insulating effect of the expandable graphite results in lower pyrolysis temperatures and therefore in incomplete decomposition. Of course, the resulting decreased mass loss or fuel support, respectively, result in a decreasing THR.

Furthermore, the heat release per mass loss is clearly changed by the addition of ammonium polyphosphate and expandable graphite, respectively, which is shown in Fig. 5. Two effects can be proposed as the cause of the change in heat release per mass loss: first, the dilution of volatile decomposition products with incombustible decomposition products. Obviously, ammonia and water can be expected as incombustible decomposition products for ammonium polyphosphates, whereas water and sulphur dioxide are the expected products of expandable graphite. The volatile components of the expandable graphite yield at least around 3 wt% and around 4 wt% with respect to the initial sample weight of incombustible volatiles for V5 G15 and V5 G25, respectively. Secondly, the different values for heat release per mass loss are due to the differences in the effective heats of combustion characteristic for the different matrix materials. This difference is caused by the changed ratio of the flax to the PP content. The two compounds are characterized by quite different net heats of combustion Δh_c^l. For cellulose a net heat of combustion of 16.12 MJ kg^{-1} is reported, whereas the net heat of combustion of PP is 43.23 MJ kg^{-1} [39]. The ratio is varied mainly by the different amounts of PP content in the materials (Table 1), whereas the content of 30 wt% flax is equal for all investigated samples. In the second part of Fig. 5, the THR is plotted against the estimated heat release, considering the products of PP and flax content with their corresponding net heats of combustion. The data correlate quite well to each other and to a line through the origin with a slope of 1. The influence on the heat release per mass loss based on the different ratios of PP and flax content is dominant. However, beyond this main effect the data are a slightly, but systematically, above the line through the origin with a slope of 1. This is probably caused by the approximations, as the heat of combustion for cellulose was used rather than that for flax. Furthermore, in the case of V8 APS25 and V5 G15, no fuel or fuel like contribution from

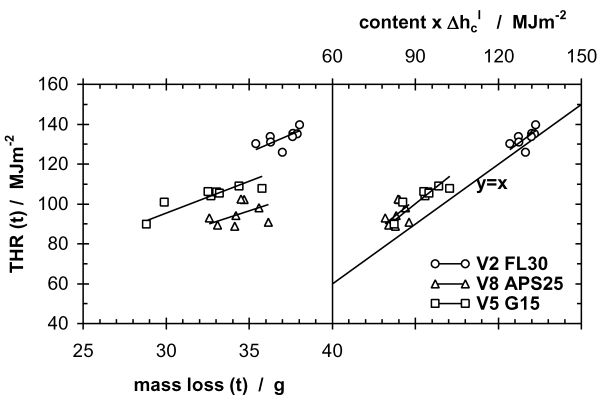

Fig. 5. Total heat release (THR) plotted against mass loss and THR plotted against the sum of the PP and flax content, multiplied by their net heat of combustions; THR and mass loss are observed for the flameout (t).

the decomposition of the fire retardants was taken into account. Such contributions cannot be totally ruled out, since for instance, the synergist for ammonium polyphosphate may cause a fuel production and the oxidation of expandable graphite may be monitored with the oxygen consumption method, respectively. In fact, there is a significantly larger deviation from the line through the origin for the samples V2 APS25 and V5 G15 than for the V2 FL30 sample.

In Fig. 6 the fire risks of samples are compared for the different external heat fluxes. The total heat evolved is plotted against peak of the heat release rate divided by time to ignition in order to classify the fire behaviour [40]. The ordinate illustrates the propensity to cause a long duration of fire, whereas the abscissa corresponds to the propensity to cause a quickly growing fire. Obviously, sufficient fire retardancy reduces both of these significantly. All the used fire retardants show in principle such an sufficient fire retardancy. Hence, a concrete demand on the fire behaviour may be fulfilled easily by adjusting the amount of fire retardant. Comparing V8 APS25 and the materials containing expandable graphite, the APP based system has advantages in terms of reducing the duration of fire for high external heat fluxes, whereas this advantage at least vanishes for low external heat fluxes, since the described additional effect of incomplete decomposition yields to an additional decrease of THR in the case of expandable graphite. Furthermore, V5 G15 and V5 G25 graphite have advantages in respect to reducing the flame spread.

3.4. Fire behaviour: flammability

Even though the cone calorimeter is called a performance based method, it is still a special fire scenario. The samples are tested in a horizontal geometry with prevented dripping

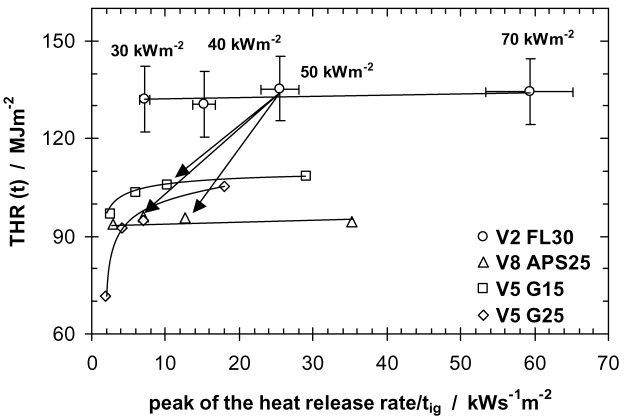

Fig. 6. Fire behaviour assessment by plotting the total heat release against the peak of the heat release rate divided by the time to ignition. The four different materials are compared for the four different external heat fluxes. Each data point is averaged for the performed measurements. The typical errors are only indicated for V2 FL30 in order to keep the clarity. The comparison of the materials for 50 kW m^{-2} is exemplarily illustrated with arrows.

under well ventilated forced flaming conditions. However, the extensive data presented in last paragraph represented in a way a comprehensive characterization of the fire response. The extrapolation of the steady heat release rate to an external heat flux of zero can be expected to correlate to the performance in flammability tests [41]. The values of the steady heat release rate were determined from cone calorimeter results of the heat release rates as defined and proposed by Lyon for thick charring, intermediate thick and thin samples [41]. The steady state heat release for the external heat flux zero is evaluated by linear extrapolation and called critical heat release rate. It is obvious that a correlation between different tests is a sophisticated challenge since the different tests simulate totally different fire scenarios. However, it is worth noting that the flammability tests UL 94 and LOI are widely accepted as important test for plastics. In sum, the V0, V1 and V2 classification according to UL 94 marks self extinguishing behaviour in the UL 94 test. The demands to reach V0 are the strongest. Flammable materials get a HB classification, if their flame propagation does not exceed a certain velocity. The LOI is used to order the flammability of materials. Normally, the materials characterized with LOI below 26–28% are flammable in other tests, whereas materials above 26–28% are self extinguishing. The test with respect to the burning behaviour of interior materials of vehicles (GMI 60261) and the glow wire test were performed with respect to probable applications of PP-flax compounds. Similar to the UL 94 also the GMI 60261 differentiates between flammable and self extinguishing materials. The glow wire test mainly targets on the ignition. In Table 3, the results are summarized for the critical heat release rate evaluated from the cone calorimeter investigation and the data for the four different flammability tests. Table 3 gives a quite comprehensive characterization of the flammability behaviour. All the data correlate well to each other. In every case, V2 FL30 is the worst, V5 G25 is the best and V5 G15 is better than V8 APS25 in terms of fire retardancy. Especially, V5 G25 shows interesting properties in respect to applications. It reaches a V1 UL 94 classification and passes the glow wire test for 1233 K.

Even though a convincing correlations are found between the steady heat release rate obtained from the cone calorimeter data and the flammability test results, our results do not offer a straightforward agreement to previous reported comparisons between cone calorimeter data and flammability tests. Different critical heat release rates of 96 ± 10 kW m^{-2} and 125 ± 25 kW m^{-2}, respectively, are reported, marking the transition to self extinguishing behaviour [37,41,42]. Hence, even V5 G15 should achieve a V classification in the UL 94 test and V5 G25 should be classified as V0, but neither is the case. The authors assume that the conversion to loose ash falling off the samples must be considered as analogous to dripping material. In fact, losing parts of the intumescent char due to the expandable graphite is equated with losing fire retardancy. Consequently,

Table 3
Flammability of the different materials determined using the steady heat release rate of the cone calorimeter, LOI, UL94, GMI 60261 and IEC 695 (2-1)

Sample	Critical heat release rate (kW m^{-2})	LOI (%)	UL 94	GMI 60261 (mm min^{-1})	IEC 695 (2-1) (K)
V2 FL30	167 ± 15	21	HB	35	923
V8 APS25	131 ± 15	26	HB	0, SENBR	1023
V5 G15	73 ± 15	29	HB	0, SENBR	1123
V5 G25	35 ± 15	30	V1	0, SENBR	1233

SENBR = self extinguishing no burn rate.

the transition of the horizontal cone calorimeter test to vertical test geometry is not admissible.

3.5. Fire behaviour: fire hazards for the forced flaming conditions in the cone calorimeter

Beyond the burning characteristics discussed in the previous paragraphs, the evolution of CO and smoke are the most important hazard to life during a fire and are discussed in the following using the term: fire hazards. Adding reasonable amounts of ammonium polyphosphate or expandable graphite afford the opportunity to decrease fire hazards in manifold ways. The amount of combustible material is decreased by simple replacement and furthermore the char formation of the polymer matrix can be enhanced. So, for instance, for polyurethane systems both ammonium polyphosphate and expandable graphite are reported, reducing the production of toxic gases such as CO and HCN, smoke, weight loss and the formation of soot [43]. For that matter, expandable graphite enables a decrease in toxic gases in a lower proportion than ammonium polyphosphate does in polyurethane.

During the cone calorimeter experiment, the fire hazards' smoke and CO production were monitored. Fig. 7 shows the total smoke production and the six-minute (after ignition) CO yield average, which is representative for the burning, for the different materials and external heat fluxes. The behaviour of smoke and CO production is qualitatively so

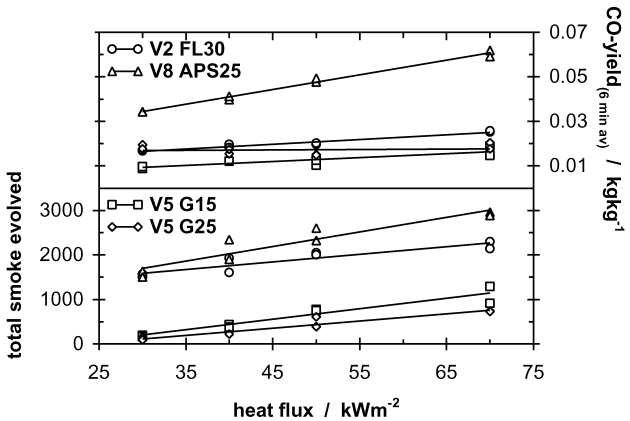

Fig. 7. Total smoke evolved and the CO yield averaged for the 6 min after the time to ignition (CO-$yield_{(6\ min\ av)}$) plotted against the external heat flux.

similar, that Fig. 7 adequately summarizes the results in respect to absolute production and yield for both. The ammonium polyphosphate system exhibits an increased smoke and CO production per mass loss. The increase in fire hazards caused by a higher fire hazard per mass loss exceeds the reduction based on the diminished mass loss. Consequently, the samples for V8 APS25 show an increase of fire hazards. It becomes clear that the fire retardancy in terms of fire risks must be paid by an increase in fire hazards with respect to forced flaming conditions. The V5 G15 and V5 G25 systems show a reduction in the smoke and the CO production per mass loss. Since the compounds are also characterized by a diminished mass loss, an effective reduction of fire risks and fire hazards is realized simultaneously.

4. Conclusion

The thermal behaviour of the materials was studied with thermogravimetric experiments. All materials show two decomposition steps. Using FTIR evolved gas analysis, the steps in the mass loss were assigned to the distinct decomposition processes of the different compounds. The fire response was characterized with cone calorimeter investigations and the products were ranked according to their performance in terms of fire risks and fire hazards. In terms of peak of the heat release, the fire retardancy increases in the order V8 APS25, V5 G15 and V5 G25 in comparison to V2 FL30. In terms of fire hazards such as CO and smoke production, V8 APS25 shows an increase whereas V5 G15 and V5 G25 shows an increasingly improvement with increasing amount of expandable graphite. The variation of the external heat flux in the cone calorimeter delivers a comprehensive characterization of the fire response for forced flaming combustion. Four different flammability tests, LOI, UL 94, GMI 60261, glow wire test, which are important for plastics and for applications in the electronics and for vehicles, were performed to characterize the flammability behaviour. The performance of the materials can be ranked in the order: V5 G25, V5 G15, V8 APS25 and V2 FL30. The extrapolation of the steady heat release rate to an external heat flux of zero was used to compare the cone calorimeter results with the results obtained for the flammability tests.

Acknowledgements

Parts of the work were supported by the German Federal Ministry of Economics and Technology in the context of the research project Reg.-Nr. 1173/00.

References

[1] Jeronimidis G. In: Elices M, editor. Structural biological materials—design and structure–property relationship. Amsterdam: Pergamon Press; 2000. p. 1–29. Chapters 1 and 2.
[2] Savage D. Biopolymers: sophisticated materials with growing market potential, 2nd ed. New York: Wiley; 1998.
[3] Rowell R, Young RA, Rowell JK, editors. Paper and composites from agro-based resources. Boca Raton: CRC Press Lewis Publishers; 1996.
[4] Schartel B, Wendling J, Wendorff JH. Macromolecules 1996;29: 1521–7.
[5] Saheb DN, Jog JP. Adv Polym Technol 1999;18:351–63.
[6] Riedel U, Nickel J. Angew Makromol Chem 1999;272:34–40.
[7] Rowell RM, Sanadi AR, Caulfield DF, Jacobsen RE. Utilization of natural fibres in plastic composite: problems and opportunities. In: Leao AL, Carvalho FX, Frollini E, editors. Lignocellulosic-plastic composites. Sao Paulo: University of Sao Paulo and UNESP Publishers; 1997.
[8] Elias HG. Makromoleküle, band 4. Anwendungen von polymeren, Weinheim: Wiley–VCH; 2003.
[9] Garkhail SK, Heijenrath RWH, Peijs T. Appl Compos Mater 2000;7: 351–72.
[10] Van de Velde K, Kiekens P. Macromol Mater Engng 2001;286: 237–42.
[11] van den Oever MJA, Bos HL, van Kemenade MJJM. Appl Compos Mater 2000;7:387–402.
[12] Helwig M, Paukszta D. Mol Cryst Liq Cryst 2000;354:961–8.
[13] Schwarz U, Pflug G, Reinemann S. Kunstst-Plast Eur 2002;92:93–4.
[14] Green J. Phosphorus-containing flame retardants. In: Grand AF, Wilkie CA, editors. Fire retardancy of polymeric materials. New York: Marcel Dekker Inc.; 2000. p. 147–70. Chapter 5.
[15] Horrocks AR. Textiles. In: Horrocks AR, Price D, editors. Fire retardant materials. Cambridge: Woodhead Publishing Limited; 2001. p. 128–81. Chapter 4.
[16] Camino G, Costa L, Trossarelli L. Polym Degrad Stab 1984;7:25–31.
[17] Le Bras M, Camino G, Bourbigot S, Delobel R, editors. Fire retardancy of polymers, the use of intumescence. Cambridge: The Royal Society of Chemistry; 1998.
[18] Montaudo G, Scamporrino E, Puglisi C, Vitalini D. J Appl Polym Sci 1985;30:1449–60.
[19] Schilling B. Kunstst-Plast Eur 1997;87:1004–6.
[20] Lewin M, Atlas SM, Pearce EM, editors. Flame-retardant polymeric materials. New York: Plenum Press; 1975. Chapter 1.
[21] Hummel DO, 2nd ed. Atlas of polymer and plastics analysis, vol. 2. Weinheim: Wiley–VCH; 1988.
[22] Tsuchiya Y, Sumi KJ. Appl Polym Sci 1970;14:2003–13.
[23] Li S, Lyons-Hart J, Banyasz J, Shafer K. Fuel 2001;80:1809–17.
[24] Tsuchiya Y, Sumi K. J Polym Sci: Part A-1 1969;7:1599–607.
[25] Hedrick SA, Chuang SSC. Thermochim Acta 1998;315:159–68.
[26] Statheropoulos H, Kyriakou SA. Anal Chim Acta 2000;409:203–14.
[27] Siat C, Bourbigot S, Le Bras M. Polym Degrad Stab 1997;58:303–13.
[28] Duquesne S, Le Bras M, Bourbigot S, Delobel R, Camino G, Eling B, Lindsay C, Roels T, Vezin H. J Appl Polym Sci 2001;82:3262–74.
[29] Bugajny M, Le Bras M, Bourbigot S, Delobel R. Polym Degrad Stab 1999;64:157–63.
[30] Bourbigot S, Le Bras M, Delobel R. Carbon 1995;33:283–94.
[31] Camino C, Delobel R. Intumescence. In: Grand AF, Wilkie CA, editors. Fire retardancy of polymeric materials. New York: Marcel Dekker Inc.; 2000. p. 217–43. Chapter 7.
[32] Shafizadeh F, Furneaux RH, Cochran TG, Scholl JP, Sakai Y. J Appl Polym Sci 1979;23:3525–39.
[33] Parker WJ, Tran HC. Wood materials. In: Babrauskas V, Grayson SJ, editors. Heat release in fires. Barking: Elsevier; 1992. p. 331–72. Chapter 4.
[34] Schartel B, Kunze R, Neubert D. J Appl Polym Sci 2002;83:2060–71.
[35] Schartel B, Kunze R, Neubert D, Braun U. Mechanistic studies on PA-66 fire retarded with red phosphorus. In: Lewin M, editor. Proceedings of the conference on recent advances in flame retardancy of polymeric materials, vol. 13. Norwalk: Business Communications Co., Inc.; 2002. p. 93–103.
[36] Staggs JEJ. Polym Degrad Stab 2001;74:433–9.
[37] Schartel B, Braun U. e-Polymers 2003; art. no. 13.
[38] Lyon RE. Fire Mater 2000;24:179–86.
[39] Babrauskas V. Related quantities (a) heat of combustion and potential heat. In: Babrauskas V, Grayson SJ, editors. Heat release in fires. Barking: Elsevier; 1992. p. 207–23. Chapter 8 (a).
[40] Petrella RV. J Fire Sci 1994;12:14–43.
[41] Lyon RE. Ignition resistance of plastics. In: Lewin M, editor. Recent advances in flame retardancy of polymers, vol. 13. Norwalk: Business Communications Co., Inc.; 2002. p. 14–25.
[42] Tewarson A. Generation of heat and chemical compounds in fires, 2nd ed. SFPE handbook of fire protection engineering; 1995. p. 53–124.
[43] Duquesne S, Le Bras M, Bourbigot S, Delobel R, Poutch F, Camino G, Eling B, Lindsay C, Roels T. J Fire Sci 2000;18:456–82.